610456

Final Report for
NASA Grant NAG5-8721
Joint U.S./Russian Research in Space Science Program (JURRISS)

Small impacts on Mars: Atmospheric effects

submitted by

Ronald Greeley
Department of Geological Sciences
Arizona State University
PO Box 871404
Tempe AZ 85287-1404

and

Ivan V. Nemtchinov
Institute for Dynamics of Geospheres RAS
Leninsky prospect 38, Building 6
Moscow 117979 Russia

October 28, 2002

The objectives of this investigation were to study the interaction of the atmosphere with the surface of Mars through the impact of small objects that would generate dust and set the dust into motion in the atmosphere. The approach involved numerical simulations of impacts and experiments under con trolled conditions.

The principal results are:

Numerical simulations of meteoroid entry into the atmosphere, their deceleration, ablation and disintegration due to aerodynamic, forces and subsequent impact onto the surface have been conducted for various meteoroid sizes, and velocities.

1. Meteoroids with radii of about 5 m and larger decelerate little in the Martian atmosphere and hit the surface with typical energies for meteoroids with radii 5, 20 and 100 m equivalent to the energy of 60 kt, 4 Mt and 500 Mt TNT respectively. The mass of the dust injected into the atmosphere exceeds the mass of the impactor by an order of magnitude. The dust cloud rises to high altitudes (as an example, it rises to 10 km, 20 km and 25 km at moments of 30 s, 20 s and 60 s respectively for a 100 m impactor). For all the impactors with radii less than 100 m the main energy remains in the atmosphere.

2. Direct impact by large meteoroids on Mars is rare (impacts of 5-m, 20-m and 100 m meteoroids occurs on Mars every 2-4 years, once in about 300-800 years and once 5000 - 20,000 years respectively).

3. The velocities of the impulsive wind created by the impact-generated shock waves is well above the dust threshold. For example, the impulsive wind velocity is about 200 m/s at a distance of 2.5 km from the crater produced by a meteoroid with a radius of 20 m or at a distance of 0.5 km from the crater created by meteoroids with radius of 5 m.

4. The fate of smaller meteoroids (radius of 3 m and less) substantially depends on their strength. Typically such meteoroids release energy in the air above the surface. For a 1 m meteoroid, the mass of dust lifted into the atmosphere is > 1 t, larger than the mass of a typical dust devils. Meteoroids with radii of 3 m impact Mars 1-2 times per year; radii of 1 m - about 10-20 times a year.

5. Meteoroids < 1 m mainly fragment in the atmosphere and are rather numerous (the number of impacts with sizes of 0.2 m is about 3000-10,000 per year).

6. Numerical simulations enable the shape and size of the dust cloud to be modeled. The shape, size of plumes and fireballs change with the size of meteoroids, their velocity and angle of trajectory. For vertical impacts dust plumes resemble those of dust devils (mushroom-type clouds).

7. A special 3D code was developed to describe the interaction of the wind with the dust plume. Results of simulations were compared with laboratory experiments. Numerical simulations demonstrate the formation of two antisymmetrical vortices formed in the air

around the plume. These vortices may be considered as the initial rotation for impact-generated dust devils.

8. Detailed tables of thermodynamic and spectral properties of hot Martian atmosphere, meteoroid vapor, and Martian soil vapor and developed radiation hydrodynamic codes allow the determination of radiation signatures of impacts. For large impactors the radiation energy is mainly released in the phase of plume expansion from the ground. For small impactors the radiation energy is mainly released during entry through the atmosphere and its disruption due to aerodynamic forces. Thus, the shape of light curves of Martian bolides is similar to that of terrestrial bolides, but the altitude of the meteoroid fragmentation is lower than in the Earth atmosphere by about 30 km.

9. Preliminary estimates show that electrification of the impact-generated dust cloud may influence the distribution of particles by sizes. Electric signatures created by impacts could help in detecting impacts from Martian rovers and orbiters.

Details of some of these results are given in the attached publication:

2002, Atmospheric disturbances and radiation impulses caused by large-meteoroid impacts in the surface of Mars, *Solary System Res., 36(3)*, 175-192, Kosarev, I.B., T.V. Losseva, I.V. Nemtchinov, V.V. Shuvalov, and R. Greeley.

Solar System Research, Vol. 36, No. 3, 2002, pp. 175–192. Translated from Astronomicheskii Vestnik, Vol. 36, No. 3, 2002, pp. 195–212.

Atmospheric Disturbances and Radiation Impulses Caused by Large-Meteoroid Impacts on the Surface of Mars. I. Formation and Evolution of Dust Cloud

I. B. Kosarev,* T. V. Losseva,* I. V. Nemtchinov, * V. V. Shuvalov,* and R. Greeley**

**Institute of Geosphere Dynamics, Russian Academy of Sciences, Leninskii pr. 38-6, Moscow, 117334 Russia*
***Department of Geology, Arizona State University, Tempe, Box 871404, Arizona;*
e-mail: Greeley@asu.edu

Received February 22, 2001; in final form, November 22, 2001

Abstract—We consider the mechanisms of the formation of dust ejected from craters produced by large-meteoroid impacts on the Martian surface, as well as the mechanisms of the elevation of dust that already existed on the surface, due to impulsed aeolian processes. Detailed numerical calculations of the dust injection, the shock wave propagation, and the formation and evolution of the dust cloud are carried out for vertical impacts of meteoroids with sizes from 1 m to 100 m. The results of these calculations show that dust raised by a 1-m impactor is sufficient to produce a local dust storm, while the mass of dust formed in impacts of large bodies is comparable to the mass of a regional or even a global dust storm. The impact detection rates for 1-, 5-, 20-, and 100-m-sized meteoroids are estimated to be a few impact events per year, one event in every 5–6 years, one event in every 300–800 years, and one event in every 5000–20000 years, respectively. In the last case, the thickness of the global layer of precipitated dust and small fragments, which has been formed through impacts over a period of 10^7–10^8 years, is comparable to the thickness of the global dust layer on the Martian surface. In the first case, the mass of raised dust is greater than that for typical "dust devils." The speed of impulsed wind at large distances from the impact site is shown to exceed the critical speed at which the blowing-off of dust from the surface begins. Some factors that may enhance the dust ejection have been previously ignored in numerical calculations. We discuss here the role of these factors. The second part of our study deals with the determination of the impact-induced radiation impulse and the estimation of its effect on the rise of dust.

INTRODUCTION

Impacts of planetesimals have played an important role in forming the atmospheres of terrestrial planets during the period of heavy bombardment of the inner Solar System (see, e.g., Ahrens *et al.*, 1989; Hunten *et al.*, 1989; Melosh, 1994), i.e., 0.5–1 billion years after the formation of planets of the Solar System. Later, impacts of asteroids and comets occurred with a lower frequency. However, even now they may have a serious effect on the evolution of planetary atmospheres.

At present, Mars is a cold and extremely dry planet (Zurek, 1992; Schofield *et al.*, 1997). However, space flights to Mars showed that at one time its atmosphere was probably much denser and wetter than it is in the current epoch (Pollack *et al.*, 1987; Owen, 1992; Fanale *et al.*, 1992; Hunten, 1993; Nelson and Greeley, 1999). Valleys similar to river valleys exist on Mars. Sand and dust might have been formed earlier as a result of erosion caused by moving water and glaciers or by the weathering of rocks similar to that observed on Earth. Another piece of evidence for the past existence of water on Mars is the presence of clear-cut terraces of sedimentary deposits, which have been revealed in photographs acquired by orbital stations with the help of high-resolution cameras (Malin and Edgett, 2000). These terraces are normally associated with the shores of lakes that have gradually dried up or shallow seas. However, there are other explanations for the origin of these sedimentary deposits, namely, volcanic ash, or dust and fragments produced by meteoroid impacts, or a joint action of all these factors. The question of how much new dust can arise during meteoroid impacts remains to be clarified, and this is one of the problems we solve in this study.

The study of the ejection and precipitation of dust and fragments after meteoroid impacts is of considerable interest in this and other aspects, for example, in connection with the problem of the origin of dust storms on Mars (Rybakov *et al.*, 1997).

According to the laboratory experiments performed by Greeley *et al.* (1980; 1992), the typical wind velocity required to raise dust from a flat surface covered by 20–600 μm dust grains is equal to 80–170 m/s. For the surface covered by agglutinate particles and small "pebbles," the characteristic wind velocity is 25–60 m/s at a pressure of about 5 mbars.

0038-0946/02/3603-0175$27.00 © 2002 MAIK "Nauka/Interperiodica"

The characteristic wind velocities on the Martian surface at the *Viking Lander-2* landing site during the period preceding the onset of the 1977 global dust storm did not exceed 8–16 m/s (Zurek, 1992). The dust elevation mechanism on Mars with such low wind velocities is the most incomprehensible aeolian process.

The traditional explanation is to assume that the rise of dust is initiated by the eddy structures ("dust devils") that originate in the unstable atmosphere (Greeley *et al.*, 1981; Ryan and Lucich, 1983; Kahn *et al.*, 1992; Rennó *et al.*, 1998; Fernandez, 1998; Metzger *et al.*, 1999; Barnes, 1999; Metzger, 1999; Murphy, 1999). This rise is enhanced by the increase in air speeds on the periphery of "vertical eddies" (dust devils) and by the sucking effect at the centers of these eddies, which gradually move to a new place, thus involving new dust in the motion. Such structures have been revealed in the photographs taken at the *Mars Pathfinder* landing site. In one of the images, a column 80 m wide and 350 m in height, moving up along the slope of the Big Crater at a speed of 4.6–3.5 m/s, is clearly seen. The dust concentration (7.5×10^{-5} kg/m^3) and the total mass (about 0.7 t) contained in this largest dust devil photographed on Mars have been estimated by measuring the opacity of this column. This is a rather small value compared to the mass of dust raised during the 1977 global dust storm (430 Mt) and the mass raised during a local storm (13 Mt) (Martin, 1995). We do not reject the possibility of the combined effect of a great number of dust devils, the theoretically justified possibility of forming very large eddies (Rennó *et al.*, 1998), and the role of some other factors (regional topographic features and so on). However, this mechanism is obviously unproved. It is partly for this reason that we addressed ourselves to the study of the dust elevation mechanism in impact processes as an alternative to the dust rise in convective vortex structures (dust devils).

Some hold the view that the change in the density of the Martian atmosphere and its humidity occurred in a nonmonotone way: there may have been returns to the conditions in which water appeared again and again on the surface or in the near-surface layer. Here, we will consider only impacts on the planet's surface under atmospheric conditions close to the currently existing atmosphere, assuming that water is absent on the surface and in the near-surface layers. Analytical estimates and numerical calculations in which the sizes of meteoroids are varied within certain limits also give an idea of the role of atmospheric density.

There are many possible reasons for the change in the Martian climate (Kasting and Toon, 1989). Among them are the periodic variations in the obliquity of the Martian orbit with a characteristic scale on the order of 10^5–10^6 years (Ward, 1973; Ward *et al.*, 1974) and the change in degassing intensity and volcanic activity (Mouginis-Mark *et al.*, 1992; Owen, 1992). Finally, the Martian climate might have changed as a result of the decrease in the number of impacts of large meteoritic bodies with time. On the one hand, impacts of large meteoroids may cause the erosion of the atmosphere (Melosh and Vickery, 1989; Vickery and Melosh, 1990; Ahrens, 1993; Zahnle, 1993). On the other hand, they replenish the atmosphere by adding vapors from the meteoroid and from the material of the planet's surface (Ahrens and O'Keefe, 1987; Melosh, 1989).

According to Ahrens and O'Keefe (1987), Ahrens *et al.*, (1989), and Ahrens (1993), noticeable erosion of the planetary atmosphere begins at the "atmospheric breakthrough" due to the acceleration of the shock wave that penetrates into upper, more rarefied atmospheric layers (Kompaneets, 1960; Andriankin *et al.*, 1962; Zel'dovich and Raizer, 1966). For the Earth, such a breakthrough occurs for the impactor radius R_p = 0.5 km and the impactor energy $E_p \approx 4.5 \times 10^4$ MtTHT.

The application of the model of the breakthrough of the exponential atmosphere (Ahrens, 1993) to other planets gives the following scaling law:

$$E_p \sim H^3 \rho_{00} V_{es}^2, \quad R_p \sim \rho_{00}^{1/3} H V_{es}^{2/3},$$

where H is the scale height of the exponential atmosphere, V_{es} is the escape velocity, and ρ_{00} is the atmospheric density near the planet's surface. The H values for the Earth and Mars are not very different (8 and 11 km, respectively); the "runaway velocities" (escape velocities) differ to a greater extent (5 and 11 km/s), whereas the densities ρ_{00} differ by two orders of magnitude. Hence, we find for Mars: $R_p \sim 90$ m and $E_p \sim 250$ Mt TNT. For bodies of this size and smaller, most of the impactor energy remains in the atmosphere, causing its strong disturbance.

A considerable loss of the atmospheric mass due to its expulsion by the vapors of the meteoroid and surface layers of the planet occurs for Mars, according to Melosh and Vickery (1989) and Vickery and Melosh (1990), at much higher impactor energies, namely, at 10^6 Mt TNT, and for an impactor radius of ~1 km. Here, we will consider bodies of considerably smaller size.

Analytical or semianalytical models of the atmospheric breakthrough, which were mentioned above, as well as some numerical calculations (see, e.g., Andrushchenko *et al.*, 1981), are based on certain assumptions that include, among others, the exponential distribution of density with height and the point character of explosion, assumptions that are not justified in reality. It is necessary, therefore, to resort to numerical calculations, using the real density distribution and real laws of energy release in the atmosphere during the flight of the meteoroid and its impact on the surface.

The qualitative pattern of impact erosion of the atmosphere and the replenishment of the atmosphere by the vapors of the meteoroid and surface layers is confirmed by two-dimensional calculations made by

Shuvalov and Artemieva (2000). For the Earth, in the range of impactor sizes from 1 to 30 km and for impactor velocities from 20 to 50 km/s, the replenishment is quite substantial for both asteroids and comets, whereas atmospheric erosion is rather weak. However, the quantitative results of numerical calculations differ appreciably from estimates based on simple models. For the Earth, at impact velocities of 20 km/s and for asteroid diameters of 30, 10, 3, and 1 km, the ratios of the mass loss from the atmosphere to the impactor mass amount to 4.7×10^{-5}, 1.6×10^{-4}, 7.1×10^{-4}, and 4.3×10^{-3}, respectively. A simple scaling recalculation to Mars leads to nearly the same relative losses by mass for impactors of 3, 1, 0.3, and 0.1 km in radius. Certainly, the scaling provides only a rough estimate, showing, however, that atmospheric erosion for 1-m and 100-m meteoroids considered here is insignificant. Most of the energy and mass remains in the atmosphere, resulting in strong, and sometimes large-scale and long-term, disturbances.

At the present time, when the Martian atmosphere is rarefied, bodies of 1–5 m in size reach the surface of the "Red Planet," in fact, without disruption (Rybakov *et al.*, 1997; Nemtchinov *et al.*, 1999b; Kosarev *et al.*, 1999, 2000). Such meteoroids with kinetic energy equal to an explosion energy on the order of 0.1–10 kt TNT disintegrate at altitudes of about 25–35 km (Tagliaferri *et al.*, 1994) with a rate of about 25 events per year (Nemtchinov *et al.*, 1997). Taking into account the lower density of the Martian atmosphere, which corresponds, near the planet's surface, to the density of the terrestrial atmosphere at an altitude of about 35 km, and the lower area of the Martian surface (which is smaller than the Earth's surface area by about a factor of two), we obtain that the speed of impacts of such bodies on the Martian surface is five to ten events per year. Although the mean velocity of meteoroids impacting on the Martian surface is somewhat lower than the velocity of Earth-impacting meteoroids (Steel, 1985; Olsson-Steel, 1987; Zahnle, 1993), such meteoroids, or even slightly smaller ones, may cause strong local dust storms, which, under "favorable" conditions, may sometimes be transformed into regional or even global storms (Rybakov *et al.*, 1997; Nemtchinov *et al.*, 1999b).

THE MODEL USED FOR CALCULATING IMPACT PROCESSES. NUMERICAL MODELING OF GAS AND DUST MOTION

The physical and gasdynamic processes that occur at impacts of meteoroids on the Martian surface are considered here by means of numerical modeling. Gasdynamic calculations were carried out using the SOVA code (Shuvalov, 1999; Shuvalov *et al.*, 1999), which enables us to simulate complex multidimensional streams with the special isolation of interfaces between different "materials" (soil, vapors, atmospheric gas, etc.) and to employ different types of equations of state (presented in analytical or tabular form). We also take into account the effect of gravity.

In the calculations considered below, we used the ANEOS equations of state (Thompson and Lauson, 1972; Melosh, 1989) for the condensed phase. The equations of state and optical properties of the Martian atmosphere heated by a shock wave, as well as the equations and properties for the material of impact-evaporated near-surface layers of Martian soil and for the vapors ejected by meteoroids themselves, will be briefly outlined in the second part of this study.

Conceptually, the SOVA method is similar to the CTH method used in the USA (McGlaun *et al.*, 1990). However we cannot make a detailed comparison in view of the absence of necessary information about the American program.

In the model used in the present paper, we make provision for the conversion of deformed solid soil into a set of isolated particles. The density of the material decreases during the motion of the substance around the crater (excavation stage). At the instant when the density in a certain computational cell drops below a certain critical value ρ_{cr}, the continuous substance is replaced by a set of discrete particles (dust grains, sand particles, "pebbles") of identical mass. The initial velocity of fragments at the moment of their formation was taken to be equal to the velocity of the continuous medium at the instant of its fragmentation. Such a method has been used by Teterev (1999). Moreover, new aerosol particles may arise in the process of scattering and adiabatic cooling of the vapors of the impactor and surface layers due to condensation. These very small particles (1–10 μm in size according to Zeldovich and Raizer, 1966) move at the same velocity as the surrounding gas and can therefore be described by the continuous-medium model.

The size distribution of particles ejected from the crater was fitted to the experimental data obtained at ground nuclear and TNT explosions on rocks (Adushkin and Spivak, 1993; Arkhipov *et al.*, 1997; Solov'ev and Shuvalov, 1999). Apart from particles that were produced in impacts, fine dust grains (0.1–1 mm in size) that already existed on the Martian surface can be involved in the motion. An algorithm for calculating the elevation of dust from the surface will be described below.

In order to analyze the subsequent evolution of the cloud of particles, we considered their motion with allowance for the heat and momentum exchange with the surrounding gas. We used the method of representative markers, each describing the motion of a large number of particles (10^5–10^{11}, depending on their size) with equal velocities, temperatures, and trajectories

(Teterev, 1999). The typical number of such representatives was 10^4–10^5. A special algorithm (Shuvalov, 1999) provided the determination of trajectories and velocities for large fragments, which meet almost no resistance and move along purely ballistic trajectories, as well as for microparticles moving with the local velocity of the gas flow. This method also allows the determination of the dust sedimentation rate due to gravitation, which depends on particle size. Note that the characteristic time of relaxation (equalization) of the velocities of large fragments and microparticles, τ_r, is given by

$$\tau_r = \frac{d\rho_s}{u\rho_g}, \quad (1)$$

where d is the size of particles, ρ_g is the gas density, ρ_s is the number density of particles, and u is the characteristic gas velocity. For the characteristic values $u = 1$ km/s, $\rho_s = 2.5$ g/cm^3, and $\rho_g = 10^{-5}$ g/cm^3, the times τ_r are equal to 0.01, 0.1, 1, and 10 s for $d = 0.01$, 0.1, 1, and 10 cm, respectively.

It is evident that, for small dust grains ($d = 0.01$–1 cm), the time of velocity relaxation may be comparable to the time of the expansion of the plume for a meteoroid and crater of moderate size. In this case, a strong interaction exists between dust and gas. Dust and particles move at nearly identical velocity. Near the crater, the mass of ejected material exceeds the air mass, and dust is hardly braked at all. As the plume size increases (with time or with an increase in the impactor size), the role of braking in the atmosphere is increased. However, for very large impactors, the atmospheric breakthrough occurs virtually without braking.

In the case of a meteoroid impact on rock, the sizes of fragments may be large enough—several centimeters or more for 1- to 10-m bodies. Such large fragments travel appreciable distances (several kilometers or even greater) without substantial braking.

It should be kept in mind that, apart from the substance ejected from the crater to fairly high altitudes in the form of separate fragments and dust, which then precipitate at sufficiently large distances from the impact point, so-called continuous ejecta mantles also arise. They are formed near the crater, predominantly in the zone extending from the rim crest for distances on the order of one to two crater radii (Melosh, 1989). Since this substance moves at comparatively low speed, the atmospheric disturbances are also small, and we therefore do not consider these processes here and, even less so, the subsequent modification of the crater.

The computational algorithm was tested by comparing results with experimental data, in particular with the data on a 500-t TNT ground explosion on Novaya Zemlya (Solov'ev and Shuvalov, 1999) and on some ground nuclear explosions (Adushkin and Spivak, 1993; Adushkin *et al.*, 1998), including the stage of dust precipitation (Trubetskaya and Shuvalov, 1994).

RESULTS OF CALCULATIONS OF THE IMPACT OF A 5-M BODY

For meter-sized and smaller bodies, ablation and fragmentation in the atmosphere, as well as the braking of these bodies and their fragments, are of great importance. Larger bodies, e.g., 5-m-sized bodies, reach the Martian surface almost without braking and disruption (Rybakov *et al.*, 1997; Nemtchinov *et al.*, 1999b; Artemieva and Shuvalov, 2001). The results of the numerical modeling of the impacts of cosmic bodies were briefly described by Kosarev *et al.* (1999) and Nemtchinov *et al.* (2000, 2001). These investigators considered the vertical impacts of bodies 5, 20, and 100 m in radius moving with the same velocity, namely, 20 km/s. Here, we discuss these results in greater detail.

In the first case, it was assumed that the surface is covered by a thick layer of fine dust; however, the role of the porosity of the body, which facilitates evaporation, was ignored. The results of the calculation for this case showed that the soil ejection rate at the initial stage of crater formation (within 10–20 ms of the impact for a body 5 m in radius) is 1–3 km/s. The velocity of vapor corresponding to this stage is equal to 10 km/s. The calculations also showed that the "curtain" formed from ejected soil strongly affects the stream in accordance with estimates and laboratory experiments (Schultz and Gault, 1979; Schultz, 1992; Melosh, 1994; Barnouin-Jha and Schultz, 1998).

The braking of a dense vapor in air is responsible for the development of Rayleigh–Taylor instability at the cloud boundary. This instability leads to the formation of large-scale eddies and to the mixing of dust and atmospheric gas. Within 200–300 ms of the impact, a jet of the impactor material carves through the target-vapor cloud. Later on, the entire mass of the meteoroid emerges from the crater.

The results of the calculation of the distribution of the density of gas and dust grains at a time instant 3 s after the impact of a 5-m body are shown in Fig. 1. Dots on the right are the markers that represent dust fragments. At this instant of time, the atmospheric inhomogeneity scarcely affects the results of the calculation, because the shock wave and the cloud of dust and vapor rise only about 2.5 km above the surface.

The parameters of the vapor cloud were calculated also for the impact of a body on a rocky surface. For large fragments, the ejection process resembles that of the case in which dust is completely ignored, because fragments interact only slightly with surrounding air. In the case of an impact on a thick dust layer, the plume geometry is largely determined by the moving dust.

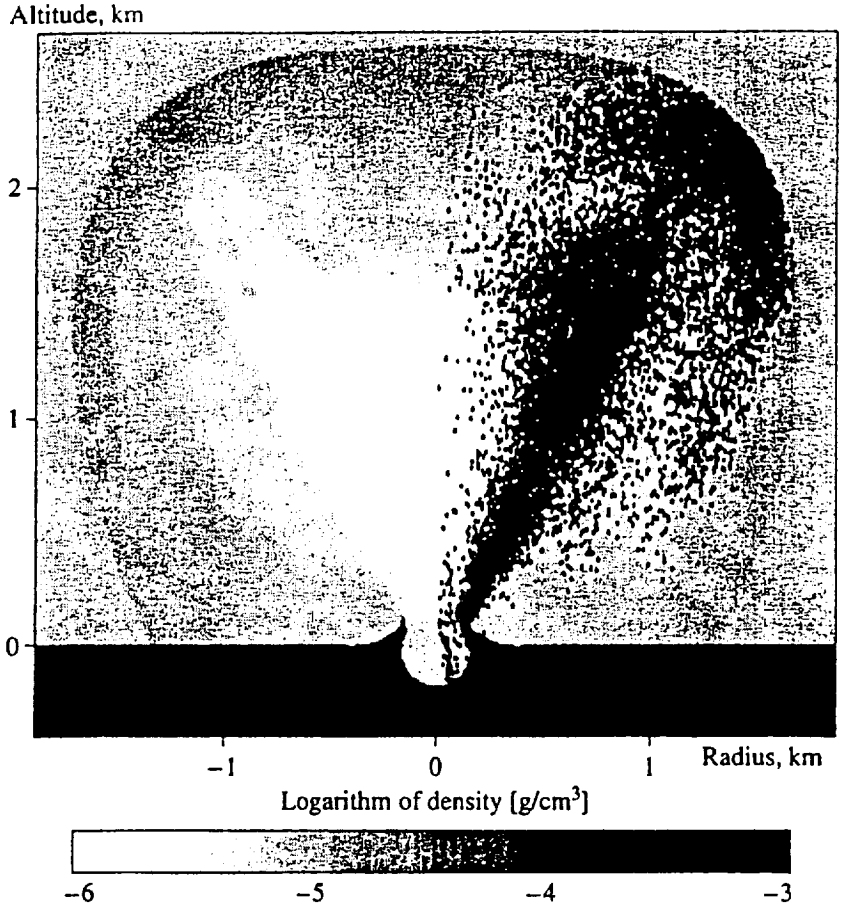

Fig. 1. The distribution of the density of gas and dust particles 3 s after the impact of a meteoroid of radius 5 m at a speed of 20 km/s.

The shape of the vapor cloud coincides with the shape of the dust "curtain."

Analysis of the dust cloud for both impact variants at later instants of time showed that the ultimate results are close to each other. At the later phase, the evolution of the cloud is largely determined by the Archimedean force and turbulent mixing. The dust cloud rises about 10 km. Its horizontal size reaches several kilometers. Within 300 s of the impact, the mass of dust involved in motion is equal to 60 M_0, if the impactor with mass M_0 hits the dust layer, and equals 10 M_0 in the case of an impact on a rocky surface. Thus, for a 5-m impactor (i.e., for an impactor with mass equal to 1.3×10^3 t), the mass of injected dust comprises 1.3×10^4–8×10^4 t. In both cases, 5 min after the impact, the cloud is not transparent for incident solar radiation.

Observations in the regions of the *Viking* and *Mars Pathfinder* landing sites did not show the presence of a thick dust layer. However, observations made from orbiters indicate that dust clustering (with a mean thickness of 1–6 m) takes place in some regions, for example, in dunes of up to 10–20 m in height, with a mean distance between neighboring dunes of 500 to 2400 m (Christensen and Moore, 1992; Greeley *et al.*, 1992; Parker and Rice, 1997). In some craters, the dust layer also appears to be sufficiently thick. On average, however, the dust layer is apparently not very thick. As to the stratified deposits of sedimentary rocks on Mars, which may have a significant thickness (that is, they may completely fill, up to the crests, rather large craters up to 200 km in size), their density, structure, and other properties are virtually unknown, except that these deposits are likely to be solidified (Malin and Edgett, 2000; Edgett and Malin, 2000). In view of this, we will henceforth use only the calculations of ejection corresponding to the impact on rocky material. The possible role of water and ice will be briefly discussed below.

Another factor that may influence the evolution of the dust cloud is the wake that follows the meteoroid during its flight through the atmosphere. Expanding vapor experiences lower resistance in a rarefied wake (Nemtchinov and Shuvalov, 1992); the latter can be considered as a kind of half-empty tube. In the case of

an impact on the dust layer, the stream proves to be essentially anisotropic if the wake is taken into account. In 300 ms, the shock wave induced by the explosion covers in the wake twice the distance that it does outside the wake. At the 30-s point, the upper boundary of the shock wave reaches an altitude of ~15 km, and the dust cloud reaches an altitude of 10 km. Within 300 s of the impact, this cloud rises 15 km above the surface. However, only a small portion of the dust moves within the wake. As a result, the mass of dust in the plume turns out to be nearly the same as when there is no wake.

IMPACT OF A 1-M METEOROID

In the case of an impact on a rocky surface, the results of the calculation for a body of one size can be approximately recalculated for the body of another size on the basis of the geometric similarity: the sizes of the plume, crater (at the stage of its formation and excavation), fragments, shock wave, and wake, as well as all characteristic times, are proportional to the impactor size, whereas pressure, velocities, densities, and temperatures remain unchanged. This is approximately valid for moderate-sized bodies and up to certain instants of time, as long as the plume and the entire disturbed region develop in a uniform atmosphere (the characteristic dimensions of which are less than the scale height of the atmosphere), and provided that we neglect radiation effects (the role of radiation will be considered below). For example, the results of calculations for $R = 5$ m can be recalculated for the case of the impact of a body with $R = 1$ m, if this body does not experience braking and disruption in the Martian atmosphere. The mass of injected dust within 60 s of the impact should be as high as 100 t, which is considerably greater than the mass inferred from observations of typical dust devils.

The above considerations of geometric similarity were tested by direct calculations of the corresponding problem. The dust cloud reached an altitude of ~2 km, and its horizontal size was estimated to be ~1 km. By the 100-s point, the dust cloud contains 250 t (or 25 M_0, where M_0 is the impactor mass). Thus, similarity is only approximate.

The calculations were also carried out for a lower impact velocity, namely, for 11 km/s. The cloud sizes were approximately the same, but the mass of dust was only ~80 t, or 8 M_0.

We have dealt so far with the impact of a body that was not disrupted in the atmosphere owing to its rather high strength. The ejection of particles from the growing crater was assumed to be the major source of raised dust, which is also the case for contact nuclear and TNT explosions. However, in the case of contact explosions, a considerable portion of dust can be raised behind the shock wave (Glasstone and Dolan, 1977; Adushkin and Spivak, 1993). Simple estimates (Nemtchinov *et al.*, 1999a, 1999b) show that in many cases relatively small bodies (of about 1 m in size) may actually be destroyed, braked, and may release energy mostly over the surface. We carried out calculations for the case where energy release occurs at a high rate and the development of the disturbed region resembles that of an explosion in air (Glasstone and Dolan, 1977) (Dust, which already existed on the surface, is blown away by air moving behind the shock wave, and the elevation of dust occurs in convective streams that originate during the rise of the hot region). These processes are similar in many respects to those that occur in the case of surface erosion by natural winds (Greeley and Iversen, 1985; Greeley *et al.*, 2000a).

Comparison with nuclear explosions set off near the Earth's surface (Glasstone and Dolan, 1977) shows that "wind erosion" dominates when the explosion is made at a relative altitude of 900 m/kt$^{1/3}$ above the Martian surface (we took into account the lower density of the atmosphere of Mars).

Numerical Model of Rise of Dust from the Surface. The above-mentioned SOVA code (Shuvalov, 1999) was used to model the rise of dust, which already exists on the surface, caused by impulsed winds. However, in contrast to the previous calculations, we used the Navier–Stokes equations instead of the Euler equations. This is necessary in order to take into account turbulent viscosity and diffusion. We used the viscosity coefficient ν and the diffusivity D in the following form:

$$\nu \times D = 0.2V^2.$$

Here ν and D are given in m^2/s and the flow velocity V, in m/s. This relationship allows us to reasonably describe the origination and evolution of the dust pedestal in large-scale explosions (Nemtchinov *et al.*, 1993; Adushkin and Nemtchinov, 1994).

To calculate the diffusive spreading of dust, we employed a Monte Carlo method. The displacement δr of a particle over the time interval τ was determined as follows:

$$\delta r = V\tau + j(6D\tau)^{1/2},$$

where j is the unit vector oriented in a random direction.

The main problem with this model was the question of how to determine the flow of dust that rises from the surface to the atmosphere. We consider an air layer with a thickness $\delta = (D\Delta t)^{1/2}$, where Δt is the time step. On the one hand, the gas velocity in this layer is determined by the velocity of the free flow. On the other, the layer is braked as a result of the entrainment of particles by the gas flow. For time Δt, new dust particles diffuse into the layer of atmospheric gas with mass $M_g = \delta\rho_0$ (per unit area) for distance δ. Braking disappears when the velocity drops below the critical velocity V_{cr} and when the blowing-away of particles stops. The momentum balance is determined by the equation

$$\alpha\delta\rho_g(V_g - V_{cr}) = \Delta M_p V_{cr},$$

where ρ_g is the air density, V_g is the air velocity, α is the blowing-away efficiency, and ΔM_p is the mass of dust particles per unit area. Dust does not penetrate into the atmosphere if $V_g < V_{cr}$.

The diffusion and upward motion of gas particles are responsible for the spreading of the dust cloud to high altitudes. At the same time, a certain amount of dust settles down owing to the action of gravity, winds, and downward diffusion from dusty layers adjacent to the surface. However, the impact of particles on the surface leads to the rise of new dust. This "saltation" effect can be taken into account by adding the mass $\beta\Delta M_{pd}$ to the mass ΔM_p where is the specific mass of particles falling on the surface ΔM_{pd} for time Δt, and β is the saltation efficiency.

The proposed model contains several parameters: V_{cr}, α, and β. The velocity V_{cr} depends on several factors, including the surface structure, the size of dust grains, and roughness (Greeley *et al.*, 2000b). This quantity and two other constants (α, β) have been measured in numerous laboratory experiments. However, these parameters are still unknown in the natural conditions on Mars. Here, in our preliminary studies, we varied these constants to evaluate their effect on the ultimate result.

The Calculation of the Rise of Dust at the "Air Explosion" Caused by the Disintegration and Rapid Braking of a 1-m Meteoroid. The model described above was applied to the evaluation of the amount of dust in the Martian atmosphere after disintegration and rapid braking of the meteoroid with an initial size of 1 m and an initial velocity of 11 km/s at an altitude of 100 m over the surface; braking leads to a short-term release of energy equivalent to the chemical energy of a 0.15 kt TNT explosion.

The following parameters were used in one of the variants: $\alpha = 0.5$, $\beta = 0.5$, and $V_{cr} = 50$ m/s. The average size of dust grains was assumed to be 2 μm, and their density was taken to be 2.5 g/cm^2. A considerable portion of dust from the region within 1 km of the epicenter was involved in the motion. The height of the dust pedestal was 5–10 m. A fireball, very similar to that produced by a nuclear explosion, was formed (Glasstone and Dolan, 1977) and began to rise. It initially contained a negligible mass of dust. However, the vortex flow in the atmosphere, which originates during the rise of the fireball, causes the dust to move toward the epicenter and then upward. The dust column connecting the fireball with the dust pedestal is formed, and then dust from the column gradually fills up fireball, forming a toroidal cloud. During the first minute, the velocity of the dust cloud was 20–30 m/s. The mass of dust raised over the first 2 s was 35 t (or 3.5 M_0, where M_0 is the meteoroid mass). By the 15-s point, the mass of dust contained in the toroidal cloud, the dust column, and the dust pedestal comprised, respectively, 16, 6, and 6 t, and the total mass of dust reached 28 t (or 2.8 M_0).

For comparison, we point out that an explosion of equivalent power on the Earth at the same relative altitude raises a cloud of dust with a mass of about 30 t.

Erosion regions are smaller than the dust pedestal region, because the pedestal expands radially. Erosion reaches a maximum at a distance of 100–200 m from the explosion point.

We also undertook computations with other values of the parameters α, β, V_{cr}, and D. The mass of dust varies in inverse proportion to V_{cr} (in the range 20–50 m/s). The M_m value reaches 95 t for $V_{cr} = 20$ m/s.

A decrease in the turbulent diffusion and viscosity coefficients by an order of magnitude lowers the mass of raised dust by only approximately two times. A twofold change in the α coefficient and variations in the saltation coefficient β in the range 0–0.5 lead to a change in M_m of 20–30% ($M_m = 47$ t for $\alpha = 1$ and $\beta = 0.5$, and $M_m = 23$ t when $\alpha = 0.5$ and $\beta = 0$). An increase in the particle mass by an order of magnitude slightly (by 10–20%) changes the mass of raised dust.

An explosive wave also arises at the impact of an undisrupted meteoroid on the Earth's surface. In this case, detailed computations of erosion are still lacking, but the data presented above show that the mass of dust raised from the surface probably does not exceed the mass of dust ejected from the crater.

Dust clouds of conical or funnel-like shape, which rise to an altitude of 1–6 km above the surface, were revealed in high-resolution photographs obtained by *Viking Orbiter*. They were interpreted as convective vortex structures—"dust devils" (Thomas and Gierash, 1985; Greeley *et al.*, 1992). It should be noted that impact-induced dust structures have a similar shape and size.

The process of transformation of convective plumes into vortex structures (dust devils) is yet to be understood. Kuzmin *et al.* (2001) draws attention to the effects of the interaction of winds with obstacles of different type (for example, with large boulders formed, in particular, at meteoroid impacts, with crater rims, etc.). Note that the dust column ejected on impact also presents an obstacle for wind. The processes of interaction of this column with wind are substantially three-dimensional, and we contemplate investigating them in the future experimentally (in wind tunnels) and theoretically (using the 3D version of the SOVA method).

It is universally recognized that the dust storms on Mars develop under specific conditions in the atmosphere, which are close to the state of instability and favor dust motion as a result of the heating of the dust cloud by solar radiation. Recently, the possibility of developing a self-sustaining dust front caused by the collapse of a dust devil and the spreading of dense gas–dust jets over the surface was noted, especially in the presence of oblique relief (Parsons, 2000). A similar process should also take place at the collapse of an impact-induced plume. We plan to study these processes in a separate paper.

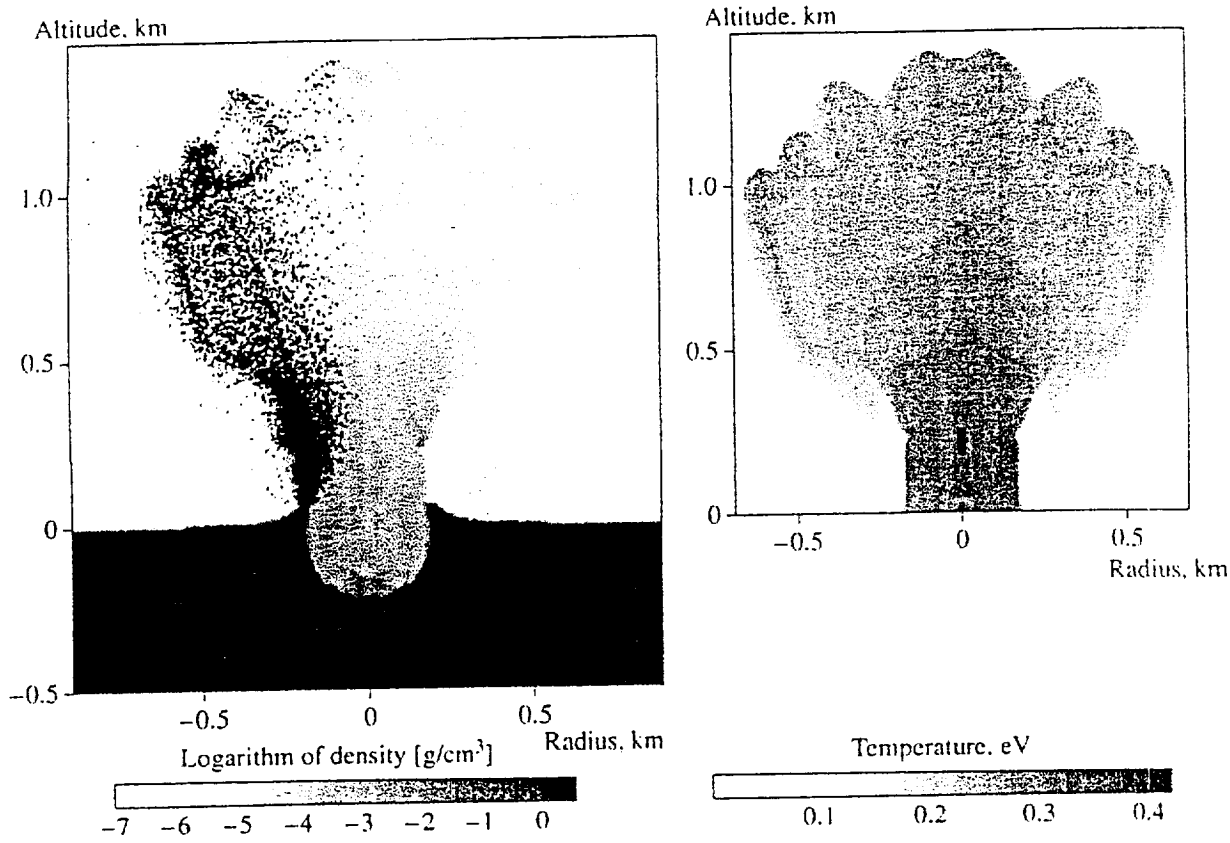

Fig. 2. The distribution of the density of gas and dust particles (left) and temperature (right) 0.3 s after the impact of a meteoroid of radius 20 m at a speed of 20 km/s.

IMPACT OF A 20-M METEOROID

We now consider the consequences of the impact of a large (20-m-sized) meteoroid on the surface at an impact velocity of 20 km/s.

The distributions of gas density and dust grains at the 0.3-s point are presented in Fig. 2. The representative markers on the left show the position of dust and fragments, as well as the distribution of air and vapor density. A large-scale turbulence caused by the development of Rayleigh–Taylor instability is clearly seen in this figure.

Similar distributions within 3 s and 10 s of the impact are shown in Figs. 3 and 4 (left). The height of the rise of the shock wave at these times is still lower than the characteristic scale height of the atmosphere. We see that most of the dust (in the upper part of the plume) moves together with the shock wave. Strictly speaking, the shock wave is almost spherical in shape, but the sphere center is raised above the surface. This is related to the fact that the kinetic energy of the meteoroid transforms initially into the energy of the compressed material of the cosmic body and the planet's surface, then partly reverts to the kinetic energy of the jet, and only later transforms into the thermal and kinetic energy of the atmosphere and vapor cloud as a result of jet braking.

The shock wave travels more slowly along the surface than above it (the maximum cross section of the disturbed region in the horizontal plane is attained within 3 s of the impact at an altitude of about 2–3 km and within 10 s of the impact at an altitude of 4–6 km.) According to Figs. 3 and 4, dust and fragments begin to fall on the surface within the spot corresponding to the radius of the cloud of 2.5–3 km before the arrival of the shock wave. In our computations, we assume that dust falling on the surface is not reflected from it and does not entrain dust that is already present on the surface. In reality, saltation of new dust grains increases the dust concentration in the near-surface layer. The gas, which moves behind the shock wave along the surface with sufficiently high speed, may entrain dust from the surface layer.

The position of the shock wave (r_s) and the gas velocity behind the wave on the surface are given in Table 1. We see that the gas velocity is considerably higher than the critical velocity leading to the rise of dust in the rarefied Martian atmosphere at distances of tens of kilometers from the impact site.

The time dependence of the gas velocity at a distance of 2.5 km from the impact site is given in Table 2. The velocity of impulsed wind exceeds the critical elevation velocity for at least 10 s.

We chose the distance 2.5 km intentionally. This is the distance between the *Mars Pathfinder* landing site and the Big Crater with diameter of 1.0–1.3 km, the greatest crater near the landing site, which is located to the southeast of this site.

Aeolian effects, including wind erosion of rocks at Rock Garden, have been analyzed by Bridges *et al.* (1999), Greeley *et al.* (1999, 2000a), Basilevsky *et al.* (1999), Golombek *et al.* (1999), and Golombek and Bridges (2000).

Rocks are largely eroded by southeasterly winds. At the same time, meteorologic data (Scchfield *et al.*, 1997; Murphey *et al.*, 1998) and the data of computations based on the global circulation model (Haberle *et al.*, 1999) indicate that the speed of such winds at the present time is, as a rule, lower than 10 m/s, i.e., it is insufficient to lift particles. Strong winds blow predominantly from the northwest (Greeley *et al.*, 1999). Hence, the conclusion was drawn that erosion is caused by paleowinds that once blew at a time of different climate (Golombek and Bridges, 2000). We put forward the hypothesis that erosion of rocks might have been caused by impulsed winds induced by a meteoroid impact. Initially, it appeared natural that it was the impact that formed the Big Crater.

However, traces of wind erosion caused by southeasterly winds were found not only on boulders at the Rock Garden, but also on the rims of 85% of the 105 craters located within an area 4.75 × 6.04 km near the *Mars Pathfinder* landing site, including the Big Crater itself (Kuzmin *et al.*, 2001). Thus, it is appropriate to analyze the possibility of impulsed wind erosion due to the impact of a larger meteoroid that may have occurred somewhat farther away to the southeast. Analysis of images of the Martian surface (similar to that performed by Kuzmin *et al.* (2001) but within a much larger area) that would indicate the possible crater–candidate is yet to be done. Here, we turn to the determination of parameters of the disturbed atmosphere and dust cloud for large meteoroids.

IMPACTS OF LARGE METEOROIDS

Let us consider the results of computations for a stony meteoroid with radius $R_0 = 100$ m and an impact velocity of 20 km/s. The impactor mass is equal to 1.3×10^7 t. The temperature and density distributions at the 10-s point are presented in Fig. 5. Dots on the left-hand side of Fig. 5 show the distribution of particles of the ejected soil material. As can be seen, the height of the conical plume at this time attains 20–25 km. The maximum height of the shock wave and shock-compressed air (indicated in gray) at this time is 25 km. According to the equation of state and the Hugoniot relations, the "air" temperature in the shock wave is low at this stage, while vapors have already cooled down considerably as a result of adiabatic expansion, and their temperature is close to the phase transition temperature due to condensation, as with the case of an impact on the Moon—a body completely devoid of atmosphere (Nemtchinov *et al.*, 1998a, 1998b). The effect of the braking and heating of vapors at the boundary of the shock-compressed layer hardly appears at all in this situation.

Parameters of the shock wave, which travels along the surface (radiative heating is ignored) are listed in Table 3. On the left, we present the data obtained for a uniform atmosphere; on the right, data for a nonuniform atmosphere. We used the values of density and temperature at different altitudes that were obtained during the descent of *Mars Pathfinder* (Magalhaes *et al.*, 1999). As can be seen, in the case of a nonuniform atmosphere, the shock-wave parameters on the surface are considerably lower than for a uniform atmosphere.

The shape of the hot region at the 10-s point differs considerably from the shape obtained for the 20-m impactor at the 2-s point. These shapes would be identical if the geometric-similarity law were valid; however, in this case the similarity law does not hold, because the height of the plume exceeds the characteristic scale height of the atmosphere.

The vapor cloud is elongated in shape. The slowing down of the plume containing the vapors of the shock-compressed layer and the related increase in temperature in the shock wave are markedly weaker than for the impact of a 20-m body. The main part of the plume has a temperature of ~0.2 eV, and a denser and hotter vapor jet exists only near the crater. The elongated shape of the plume, the increase in the cloud height, and the decrease in the cloud temperature point to a considerable violation of geometric similarity. (Otherwise, the fireball would be located somewhat closer to the surface, with the center at an altitude of about 10 km; however, our calculations demonstrate that the plume center is located at an altitude of about 12 km.)

The maximum radius of the shock wave at the 30-s point is ~30 km, i.e., the average radial velocity is ~1 km/s. As follows from Table 3, the radius of the shock wave on the Earth's surface at this point is only 15 km. However, the gas velocity behind the shock-wave front amounts to 50 m/s, i.e., exceeds the value sufficient to raise the dust. Thus, strong erosion might be expected within an extensive zone of at least 10–15 km in size during a time interval of no less than 20–30 s. We have not yet carried out detailed calculations of erosion for two reasons. First, the enormous sizes of the disturbed region and the constraints on the possible number of computational points do not allow us to conduct the calculations with a sufficiently fine step for the entire computed region, including near-surface layers; these calculations require a modification of the computational procedure, which is currently being worked

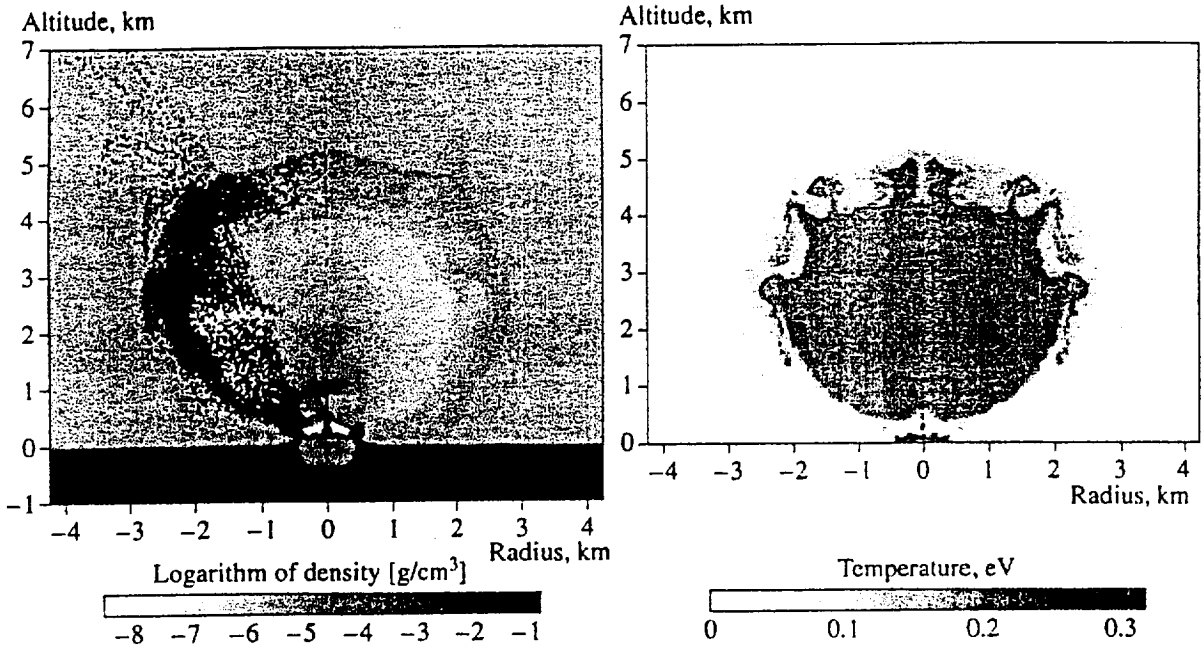

Fig. 3. The distribution of the density of gas and dust particles (left) and temperature (right) 3 s after the impact of a meteoroid of radius 20 m at a speed of 20 km/s.

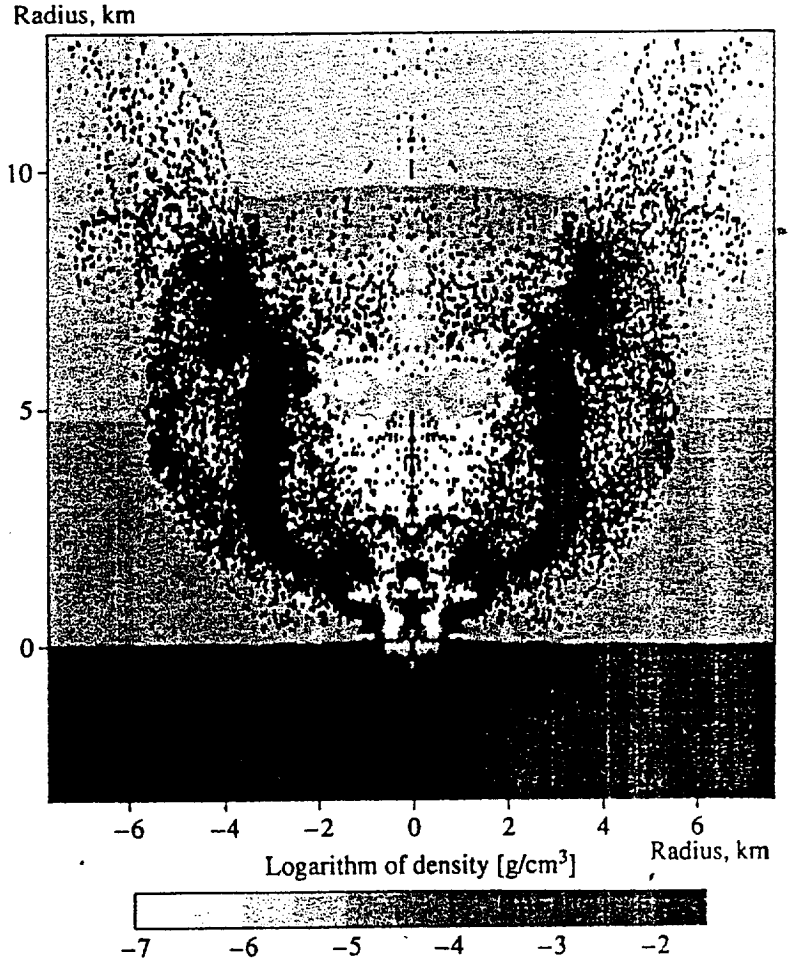

Fig. 4. The distribution of the density of gas and dust particles 10 s after the impact of a meteoroid of radius 20 m at a speed of 20 km/s.

out. Second, radiation emitted from the hot region may cause additional effects that facilitate the rise of dust. These problems will be considered in the second part of this study.

Finally, we should note that experiments are also necessary on the aeolian abrasion produced by dust particles with a higher speed and shorter duration of its action than those conducted by Kraft and Greely (2000).

At the 60-s point (Fig. 6), the shock wave reached an altitude of ~300 km, i.e., the mean velocity increased to 5 km/s and exceeded the escape velocity for Mars. As a consequence, the effect of the atmospheric breakthrough begins to manifest itself, although only a small mass possesses such a high velocity. The cone of ejection of the planet's substance reaches an altitude of 100–120 km, and the dispersion of particles occurs in an almost inertial way: the strong effect of gravity is yet not pronounced.

By the 60-s point, the cone radius increased to ~100 km (Fig. 6), which means that the maximum radial velocity of the cone even increased. As to the explosion products, their maximum radius reaches 70 km, i.e., the radial velocity is less than 1.2 km/s at a maximum height of 120 km and a vertical velocity of ~2 km/s.

The limiting height of elevation of dust and soil fragments and their radial dispersion are estimated to be ~1000 km, on the assumption that the ejecta move ballistically with the above-indicated velocities. The mass of the ejected material is equal to about 10 M_0, i.e., 10^8 t for the given meteoroid. Assuming that this material is uniformly distributed over the circle of the radius equal to this height, the average specific mass is equal to ~30 g/m^2, which corresponds to a layer thickness of ~10 μm.

The evolution of the dust cloud in the atmosphere at a later stage must be determined on the basis of global-circulation models. However, the impact of a large cosmic body can appreciably modify the global circulation as a result of the absorption of solar radiation by ejected dust and the heating of the atmosphere caused by the incident plume and the damping of oscillations.

IMPACT RATE

An extensive program of telescopic observations provides information about the distribution of 1-km and larger cosmic bodies in circumterrestrial space. According to the estimates made by Steel (1985), the mean probability of collisions in a sample of 284 asteroids crossing the orbit of Mars is 3.5×10^{-10} per year. Since there are ~ 10^4 such bodies with size > 1 km, the mean time interval between impacts is equal to 3×10^5 years. For smaller bodies, extrapolation based on the $N \sim D^{-\alpha}$ law, where $\alpha = 1.8$–2.0, and on lunar (Neukum and Ivanov, 1994) and Martian (Strom *et al.*, 1992; Ivanov, 1999) cratering data yields an impact probability equal to one impact event every 3000–5000 years for 100-m bodies and one event every 200–300 years for 20-m bodies.

Table 1. The shock wave front position (R_s) and the maximum wind velocity (u_s) as a function of time for the impact of a 20-m meteoroid

t, s	R_s, km	u_s, m/s
1	0.70	190
2	1.25	150
3	1.70	180
4	2.20	210
5	2.65	210
6	3.10	210
7	3.60	170
10	4.75	150
14	6.15	140
20	8.10	110

Table 2. Near-surface wind speeds behind the shock wave as a function of time at a distance of 2.5 km from the impact site of a meteoroid of radius 20 m

t, s	u, m/s
4	0
4.5	180
5	150
6	70
7	40

Satellite observations of flashes on the entry of meteoroids into the Earth's atmosphere provide satisfactory statistical data for bodies with sizes of up to 1–3 m (Tagliaferri *et al.*, 1994; Nemtchinov *et al.*, 1997). These data can also be used for estimates of the rate of impacts on Mars, taking into account the differences in the surface areas. Data of satellite observations for the Earth can be represented (Nemtchinov *et al.*, 1997) in the form $N^* = 7E^{-0.72}$ or $N^* \sim D^{-2.2}$, where N^* is the number of impacts per year and E is the energy in kt TNT. A stony meteoroid of radius 5 m with an impact speed of 20 km/s has a kinetic energy of about 60 kt. This value slightly exceeds the maximum energy that was detected by satellites over several years of systematic observations (40 kt TNT). The rate of impacts of such meteoroids on Earth, obtained by extrapolation of the above dependence, is one impact event every two to three years. The rate of impacts on Mars can be evaluated as half of the impact detection rate for the Earth (Adolfson *et al.*, 1996). It amounts to one impact event every five to six years.

Extrapolation to high energies is open to question, because it is in this size range that a kink in the $N^*(D)$ dependence is possible. However, using this dependence for a 20-m body, we obtain an impact detection rate of one event every 300–400 years. Smaller bodies

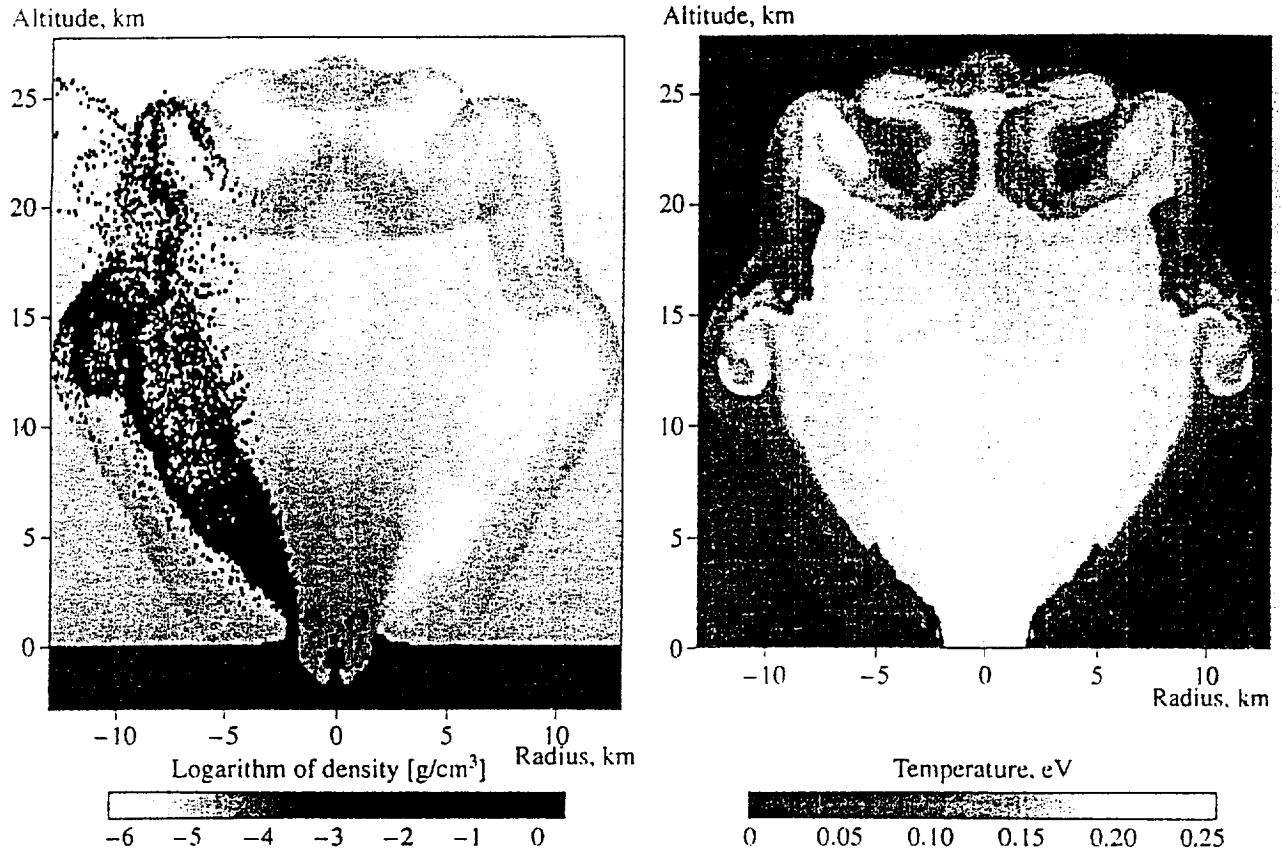

Fig. 5. The distribution of the density of gas and dust particles (left)and temperature (right) 10 s after the impact of an asteroid of radius 100 m at a speed of 20 km/s.

(e.g., those of 0.3–1 m in size) penetrate the Martian atmosphere more frequently, and for such bodies we should take into account fragmentation and braking in the atmosphere. However, even a low-altitude "explosion" may produce a local dust storm (Rybakov *et al.*, 1997; Nemtchinov *et al.*, 1999b). For larger bodies (≥1 km), such events occur more rarely and may have a strong effect on the atmospheric conditions during a long period of time.

There are different estimates of the time of transition to the "tenuous" and cold Martian atmosphere. The upper estimate (3.5–3.8 Myr ago) corresponds to the end of the period of heavy bombardment. However, there are data indicating that a dense atmosphere and humid climate existed on Mars also after this period (Pollack *et al.*, 1987). The lower estimate (50–100 Myr ago) is based on a hypothesis for recent volcanic activity on Mars (Hartmann, 1998, 2000; Hartmann and Berman, 2000; Hartmann *et al.*, 1999). Nevertheless, meteoroid impacts on Mars, which possessed an atmosphere then similar to the current one, repeatedly occurred even during this relatively short period.

Table 3. Parameters of the shock wave propagating along the surface used in the nonuniform and uniform models of the atmosphere after an impact of a meteoroid of radius 100 m

Uniform atmosphere				Nonuniform atmosphere			
t, s	R, km	U, km/s	p/p_0	t, s	R, km	U, km/s	p/p_0
2	2.7	0.85	8.4	3	2.45	0.13	3.9
6	5.6	0.56	4.2	10	6.0	0.09	2.5
20	13.2	0.33	2.4	20	11	0.06	1.7
60	28	0.16	1.55	30	15	0.05	1.6
200	68	0.11	1.37	54	24	0.04	1.5

During the period when Mars had a rarefied atmosphere (for instance, over a period of 10^7–10^8 years, when the number of impacts of cosmic bodies with a radius of ~100 m was 10^3–10^4), the overall mass of ejected fine dust grains and soil fragments reached 10^{10}–10^{11} t, which, with allowance for the Martian surface area (1.45×10^8 km^2) corresponds to the specific mass of the global layer of sediments ~ 7×10^{-3}–7×10^{-2} g/cm^2.

Precipitated dust may be swept away into other regions of the planet, especially during the period of dust storms. According to laboratory experiments performed by Greeley *et al.* (2000b), up to 1.5×10^{-7}g/cm^2 may be carried away from a unit area per unit time. In

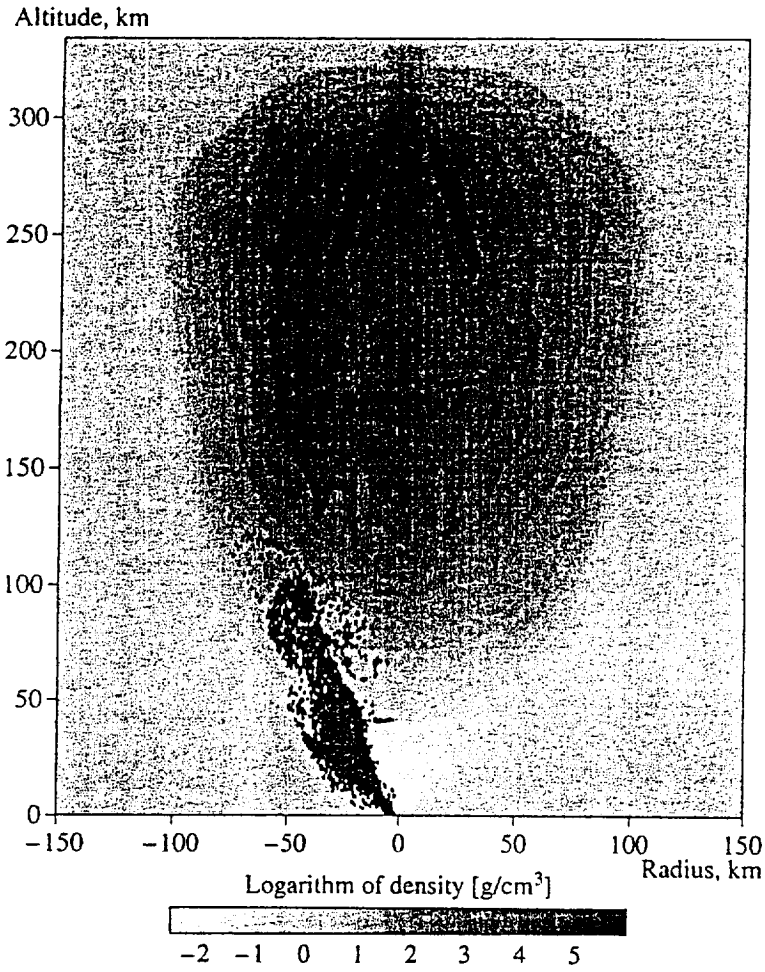

Fig. 6. The distribution of the density of gas and dust particles 60 s after the impact of an asteroid of radius 100 m at a speed of 20 km/s.

other words, the layer with specific mass on the order of 10^{-3} g/cm^2 can be transferred in one day, while the entire precipitated layer can be swept away in several days of a dust storm. Its place may be occupied by dust brought from other places. Dust precipitated on the surface is not only redistributed by winds over the surface but can be concentrated in certain places, for example, in craters and canyons. Moreover, chemical "cementation" processes decrease the mobility of "old" dust. Regretfully, these processes are insufficiently studied to provide a reliable estimate of the characteristic time of dust immobilization. Nevertheless, our data demonstrate that meteoroid impacts can explain, generally speaking, the origin of the current global dust layer on Mars.

Malin and Edgett (2000) are doubtful of the impact origin of thick layers of sediments filling some very extended regions of the Martian surface, because ejecta products must have been concentrated only near impact sites. Our calculations and estimates show that the zone of falling of dust and fragments after impacts may be sufficiently wide. Moreover, an even greater surface mass can be reprocessed by rare impacts of larger meteoroids (up to 1 km in size). We do not consider here impacts of such bodies, assuming that for them the spherical shape of the surface and atmospheric layers of the planet must be taken into account at a sufficiently early phase of evolution.

ROLE OF WATER AND ICE

When calculating impacts, we ignored the possibility of the existence of inundated and ice structures at a depth below the surface of Mars, in the Martian megaregolith (Squyres *et al.*, 1992), whose mean porosity is equal to ~25%. The characteristic depth of a porous layer on the Moon is 6.5 km. The corresponding depth for Mars is estimated to be 2.8 km. The depth of craters for the largest meteoroids considered here is on the order of, or less than, this value.

Porosity near the surface of Mars may reach 20–50% (Squires *et al.*, 1992). Over at least the first billion years, groundwater existed in the Martian crust, especially in its upper layer (megaregolith) disrupted

by impacts. At present, water apparently persists partly as ice in the cryolithosphere. On average, this amount of water is likely to match the water-layer thickness of about 100 m. Morphological features of the surface in some regions of Mars show that viscous creep of the Martian regolith is due to the deformation of ice in the soil. Based on the analysis of the structure of deposits around large craters, Squyres *et al.* (1992) arrived at the conclusion that ice-bearing layers lie at a depth of greater than 200–300 m and therefore do not affect the ejection of high-speed dust jets and fragments, which disturb the atmosphere at impacts of moderate-sized meteoroids. As to the impacts of sufficiently large meteoroids (100 m in size and larger), one should take into account the possible presence of groundwater and porosity of the surface layer in studying the processes of the formation and development of plumes and the aerodynamic processes caused by the origination of products of the disruption of the surface material in the atmosphere and by impact-induced atmospheric disturbances. These factors not only facilitate the ejection of substance at impacts (see, e.g., Stewart *et al.*, 2000), but also change the character of aeronomic processes as compared to the current processes (Barth *et al.*, 1992) involving insignificant amounts of water.

We come to the conclusion that analysis of disturbances in the Martian atmosphere caused by meteoroid impacts is far from being completed. It is necessary to take into account in greater detail the surface erosion and the elevation of dust behind the shock wave, the formation of vortex structures due to the interaction of the impact-induced shock wave with the ballistic wave that originated during the motion through the atmosphere, the upward ejection of dust due to the "explosion of the surface layer" caused by the drop in pressure in the blast wave below the initial level, the interaction of impact-induced convective plumes with the dust column arising after the impact, and some other factors. However, certain difficulties related to the lack of knowledge of the properties of the surface itself in various regions arise in this context. The necessary data can be derived from observations of impacts occurring in the current epoch. In this case, we come up against an additional problem related to the properties of impacting bodies and their braking/disruption in the atmosphere. The detection of the radiation flash by orbital stations on the entry of the meteoroid into the atmosphere and after the impact, as well as the detection of the rise of the dust cloud coupled with ground-based seismic data, might facilitate the search for fresh craters and aeolian effects around craters, as well as the analysis of images obtained.

CONCLUSIONS

1. Relatively small meteoroids reach the surface of Mars almost without disruption and braking and with much higher frequency than they reach the Earth's surface. This is related to the very rarefied Martian atmosphere. The impact detection rate for ~1-m bodies is several events per year. Bodies of 5, 20, and 100 m in size impact on the Martian surface with a frequency of one impact event every 5–6 years, every 300–800 years, and every 5000–20000 years, respectively.

2. No atmospheric breakthrough occurs after the impacts of bodies of ≤ 100 m in size. Most of the energy and mass remains in the atmosphere, leading to strong, large-scale, and sometimes global and long-term, disturbances.

3. The mass of dust entering the atmosphere at impacts of 1-m meteoroids exceeds the typical mass of a "dust devil." Impacts of bodies of about 5, 20, and 100 m in size give rise to the injection of dust with mass similar to that raised during a local, regional, or even global dust storm.

4. The main mechanism of dust entry into the atmosphere is the ejection of a newly formed dust from the growing crater and vapor condensation. However, the impulsed wind behind the front of the shock wave that travels along the surface leads to wind erosion and to the rise of the already existing dust with a mass comparable to the mass of the new dust.

5. It is shown that at considerable distances from the impact site (for a 100-m meteoroid, at distances up to 10–15 km at least) the velocity of gas particles behind the shock wave front exceeds the velocity at which dust is effectively blown away.

6. A hypothesis is put forward that the abrasive action on boulders located in the Rock Garden region and on rims around small craters near the *Mars Pathfinder* landing site, as well as near the Big Crater with a diameter of ~1 km, is caused by impulsed wind behind the shock wave front, which blew from the site of impact of a large meteoroid located to the southeast of the landing site, rather than by north-westerly paleowinds (in contrast to current northeasterly winds).

7. Some factors may cause stronger erosion than that assumed in existing computational models. This necessitates a deeper insight into the relevant processes. The second part of this study is devoted to the determination of the characteristics of the thermal radiation impulse and to the estimation of its effect on the rise of dust.

8. The formation of dust at numerous impacts of large meteoroids, which occurred over a long period (10^7–10^8 years), may explain the thickness of the current global dust layer. However, the global circulation of the atmosphere and the redistribution and immobilization of dust should be taken into account to provide a more exact answer to this question.

ACKNOWLEDGMENTS

This study was supported by an NRA 98-OSS-08 JURRISS grant.

REFERENCES

Adolfson, L.G., Gustafson, B.A.S., and Murray, C.D., The Martian Atmosphere as a Meteoroid Detector, *Icarus*, 1996, vol. 119, pp. 144–152.

Adushkin, V.V. and Spivak, A.A., *Geomekhanika krupnomasshtabnykh vzryvov* (Geomechanics of Large-Scale Explosions), Moscow: Nedra, 1993.

Adushkin, V.V. and Nemchinov, I.V., Consequences of Impacts of Cosmic Bodies on the Surface of the Earth, in *Hazards due to Comets and Asteroids*, Gehrels, T., Ed., Tucson: Univ. of Arizona Press, 1994, pp. 721–778.

Adushkin, V.V., Volobuev, N.M., Divnov, I.I., *et al.*, Radioactive Contamination of an Area during First Surface Nuclear Explosions on Semipalatinsk Proving Ground, in *Dinamicheskie processy v geosferakh pod deistviem vneshnikh i vnutrennikh potokov energii i veshchestva* (Geofizika sil'nykh vozmushchenii) (Dynamical Processes in Geospheres Caused by External and Internal Energy and Material Flows (Geophysics of Strong Disturbances), Moscow: IGD (Inst. of Geosphere Dynamics), 1998, pp. 227–240.

Andriankin, E.I., Kogan, A.M., Kompaneets, A.S., and Krainov, V.P., Spread of a Strong Explosion in a Nonuniform Atmosphere, *Prikl. Mekh. Tekh. Fiz.*, 1962, no. 6, pp. 3–7.

Andrushchenko, V.A., Kestenboim, Kh.S., and Chudov, L.A., Gas Motion Caused by a Point Explosion in a Nonuniform Atmosphere, *Izv. Akad. Nauk SSSR, Mekh. Zhidk. Gaza*, 1981, no. 6, pp. 144–151.

Ahrens, T.J. and O'Keefe, J.D., Impact on the Earth Ocean and Atmosphere, *Int. J. Impact. Engng.*, 1987, vol. 5, pp. 13–32.

Ahrens, T.J., O'Keefe, J.D., and Lange, M.A., Formation of Atmospheres during Accretion of the Terrestrial Planets, in *Origin and Evolution of Planetary and Satellite Atmospheres*, Atreya, S.K., Pollack, J.B., and Matthews, M.S., Eds., Tucson: Univ. of Arizona Press, 1989, pp. 328–385.

Ahrens, T.J., Impact Erosion of Terrestrial Planetary Atmospheres, *Ann. Rev. Earth Planet. Sci.*, 1993, vol. 21, pp. 525–555.

Arkhipov, V.N., Evterev, L.S., Zamyshlyaev, B.V., *et al.*, Mechanical Impact of Explosions on Ground Media, in *Fizika yadernogo vzryva* (Physics of Nuclear Explosion), Moscow: Fizmatlit, 1997, vol. 1, pp. 159–243.

Artemieva, N.A. and Shuvalov, V.V., Motion of a Fragmented Meteoroid through the Planetary Atmosphere, *J. Geophys. Res.*, 2001, vol. 106, no. E2, pp. 3297–3309.

Barnes, J.R., Initiation and Spread of Martian Dust Storms, *5th Int. Conf. on Mars*, July 19–24, 1999, Pasadena, CA, 1999, Abstract no. 6011.

Barnoiuin-Jha, O.S. and Schultz, P.H., Lobateness of Impact Ejecta Deposits from Atmospheric Interactions, *J. Geophys. Res.*, 1998, vol. 103, no. E11, pp. 25739–25756.

Barth, C.A., Stewart, A.I.F., Bougher, S.W., *et al.*, Aeronomy of the Current Martian Atmosphere, in *Mars*, Kieffer, H.H., Jakosky, B.M., Snyder, C.W., and Matthews, M.S., Eds., Tucson: Univ. of Arizona Press, 1992, pp. 1054–1089.

Basilevsky, A.T., Markiewicz, W.J., Thomas, N., and Keller, H.U., Morphologies of Rocks within and near the Rock Garden at the *Mars Pathfinder* Landing Site, *J. Geophys. Res.*, 1999, vol. 104, no. E4, pp. 8617–8636.

Bridges, N.T., Greeley, R., Haldemann, A.F.C., *et al.*, Ventifacts at the *Pathfinder* Landing Site, *J. Geophys. Res.*, 1999, vol. 104, no. E4, pp. 8595–8615.

Christensen, P.R. and Moore, H.J., The Martian Surface Layer, in *Mars*, Kieffer, H.H., Jakosky, B.M., Snyder, C.W., and Matthews, M.S., Eds., Tucson: Univ. of Arizona Press, 1992, pp. 686–729.

Edgett, K.S. and Malin, M.C., New Views of Mars Aeolian Activity, Materials, and Surface Properties: Three Vignettes from the *Mars Global Surveyor* Orbiter Camera, *J. Geophys. Res.*, 2000, vol. 105, no. E1, pp. 1623–1650.

Fanale, F.P., Postawko, S.E., Pollack, J.B., *et al.*, Mars: Epochal Climate Change and Volatile History, in *Mars*, Kieffer, H.H., Jakosky, B.M., Snyder, C.W., and Matthews, M.S., Eds., Tucson: Univ. of Arizona Press, 1992, pp. 1135–1179.

Fernandez, W., Martian Dust Storms: A Review, *Earth, Moon, Planets*, 1998, vol. 77, pp. 19–46.

Glasstone, S. and Dolan, P.J., *The Effects of Nuclear Weapons*, Washington, DC: GPO, 1977, pp. 125–126, 151–153.

Golombek, M.P., Moore, H.J., Haldemann, A.F.C., *et al.*, Assessment of the *Mars Pathfinder* Landing Site, *J. Geophys. Res.*, 1999, vol. 104, no. E4, pp. 8585–8594.

Golombek, M.P. and Bridges, N.T., Erosion Rates on Mars and Implications for Climate Change: Constraints from the *Pathfinder* Landing Site, *J. Geophys. Res.*, 2000, vol. 105, no. E1, pp. 1841– 1853.

Greeley, R., Leach, R., White, B.R., *et al.*, Threshold Windspeeds for Sand on Mars: Wind Tunnel Simulations, *Geophys. Res. Lett.*, 1980, vol. 7, pp. 121–124.

Greeley, R., White, B.R., Pollack, J.B., and Leach, R.N., Dust Storms on Mars: Considerations and Simulations, Geol. Soc. Am. SP-186, Boulder: Geol. Soc. Am., 1981, pp. 101–121.

Greeley, R. and Iversen, J.D., *Wind as a Geological Process on Earth, Mars, Venus, and Titan*, Cambridge: Cambridge Univ. Press., 1985.

Greeley, R., Lancaster, N., Lee, S., and Thomas, P., Martian Aeolian Processes, Sediments, and Features, in *Mars*, Kieffer, H.H., Jakosky, B.M., Snyder, C.W., and Matthews, M.S., Eds., Tucson: Univ. of Arizona Press, 1992, pp. 730–766.

Greeley, R., Kraft, M., Sullivan, R., *et al.*, Aeolian Features and Processes at the *Mars Pathfinder* Landing Site, *J. Geophys. Res.*, 1999, vol. 104, no. E4, pp. 8573–8584.

Greeley, R., Kraft, M.D., Kuzmin, R.O., and Bridges, N.T., *Mars Pathfinder* Landing Site: Evidence for Change in Wind Regime from Lander and Orbiter Data, *J. Geophys. Res.*, 2000a, vol. 105, no. E1, pp. 1829–1840.

Greeley, R.G., Wilson, G., Coquilla, R., *et al.*, Windblown Dust on Mars: Laboratory Simulations of Flux as a

Function of Surface Roughness, *Planet. Space Sci.*, 2000b, vol. 48, pp. 1349–1355.

Haberle, R.M., Joshi, M.M., Murphy, J.R., *et al.*, General Circulation Model Simulations of the *Mars Pathfinder* Atmospheric Structure Investigation/Meteorology Data, *J. Geophys. Res.*, 1999, vol. 104, no. E4, pp. 8957–8974.

Hartmann, W.K., Martian Crater Population and Obliteration Rates: First Results from *Mars Global Surveyor, Lunar Planet. Sci. Conf. XXIX*, 1998, Abstract no. 1115.

Hartmann, W.K., Malin, M., McEwen, A., *et al.*, Evidence for Recent Volcanism on Mars from Crater Counts, *Nature*, 1999, vol. 397, no. 6720, pp. 586–589.

Hartmann, W.K., Young Volcanism on Mars and Implications for Planetary Exploration, *Microsymposium 32 on Comparative Planetology*, Moscow, Vernadsky Institute of Geochemistry and Analytical Chemistry, 2000, p. 50 (Abstracts).

Hartmann, W.K. and Berman, D.C., Elysium Planitia Lava Flows: Crater Count Chronology and Geological Implications, *J. Geophys. Res.*, 2000, vol. 105, no. E6, pp. 15011–15025.

Hunten, D.M., Donahue, T.M., Walker, J.C.G., and Kasting, J.F., Escape of Atmospheres and Loss of Water, in *Origin and Evolution of Planetary and Satellite Atmospheres*, Atreya, S.K., Pollack, J.B., and Matthews, M.S., Eds., Tucson: Univ. of Arizona Press, 1989, pp. 386– 422.

Hunten, D.M., Atmospheric Evolution of the Terrestrial Planets, *Science*, 1993, vol. 259, pp. 915–926.

Ivanov, B.A., Earth as a Target: Size Distribution of Impact Craters and Asteroids, in *Fizicheskie processy v geosferakh: ikh proyavlenie i vzaimodeistvie (Geofizika sil'nykh vozmushchenii)* (Physical Processes in Geospheres: Their Manifestation and Interaction (Geophysics of Strong Disturbances), Moscow: IGD (Inst. of Geosphere Dynamics), 1999, pp. 282–291.

Kahn, R.A., Martin, T.Z., Zurek, R.W., and Lee, S.W., The Martian Dust Cycle, in *Mars*, Kieffer, H.H., Jakosky, B.M., Snyder, C.W., and Matthews, M.S., Eds., Tucson: Univ. of Arizona Press, 1992, pp. 1017–053.

Kasting, J.F. and Toon, O.B., Climate Evolution on the Terrestrial Planets, in *Origin and Evolution of Planetary and Satellite Atmospheres*, Atreya, S.K., Pollack, J.B., and Matthews, M.S., Eds., Tucson: Univ. of Arizona Press, 1989, pp. 423–449.

Kompaneets, A.S., Point Explosion in a Nonuniform Atmosphere, *Dokl. Akad. Nauk SSSR*, 1960, vol. 130, no. 5, pp. 1001–1003.

Kosarev, I.B., Nemtchinov, I.V., Popova, O.P., and Shuvalov, V.V., Dynamics and Radiation of the Martian Atmosphere under Impacts of Meteoroids with Various Sizes, *Transactions AGU, Suppl. to EOS*, 1999, vol. 80, no. 46, p. F631.

Kosarev, I.B., Nemtchinov, I.V., Rybakov, V.A., and Shuvalov, V.V., Light Flashes, Dust Clouds, and Electric Discharges Caused by Meteoroid Impacts onto Mars, *Meteoritics Planet. Sci.*, 2000, vol. 35, no. 5, Suppl., pp. A91–A92.

Kraft, M.D. and Greeley, R., Rock Coating and Aeolian Abrasion on Mars: Application to the *Pathfinder* Landing Site, *J. Geophys. Res.*, 2000, vol. 105, no. E6, pp. 15107–15116.

Kuzmin, R.O., Greeley, R., Rafkin, S.C.R., and Haberle, R., Wind-related Modification of Some Small Impact Craters on Mars, *Icarus*, 2001, vol. 153, pp. 61–70.

Magalhães, J.A., Scofield, J.T., and Seiff, A., Results of the *Mars Pathfinder* Atmospheric Structure Investigation, *J. Geophys. Res.*, 1999, vol. 104, no. E4, pp. 8943–8955.

Malin, M.C. and Edgett, K.S., Sedimentary Rocks of Early Mars, *Science*, 2000, vol. 290, pp. 1927–1937.

Martin, T.Z., Mass of Dust in the Martian Atmosphere, *J. Geophys. Res.*, 1995, vol. 100, no. E4, pp. 7509–7512.

McGlaun, J.M., Thomson, S.L., and Elrick, M.G., CTH: A Three- Dimensional Shock Wave Physics Code, *Int. J. Impact Engng*, 1990, vol. 10, pp. 351–360.

Melosh, H.J. and Vickery, A.M., Impact Erosion of the Primordial Atmosphere of Mars, *Nature*, 1989, vol. 338, no. 6215, pp. 487–490.

Melosh, H.J., *Impact Cratering: A Geologic Process*, New York: Oxford Univ. Press, 1989. Translated under the title *Obrazovanie udarnykh kraterov: geologicheskii protsess*, Moscow: Mir, 1994.

Metzger, S.M., Feeding the Mars Dust Cycle: Surface Dust Storage and Dust Devil Entrainment, *5th Int. Conf. on Mars*, July 19–24, 1999, Pasadena, CA, 1999, Abstract no. 6196.

Metzger, S.M., Carr, J.R., Johnson, J.R., *et al.*, Dust Devil Vortices Seen by the *Mars Pathfinder* Camera, *Geophys. Res. Lett.*, 1999, vol. 26, no. 18, pp. 2781–2784.

Mouginis-Mark, P.J., Wilson, L., and Zuber, M.T., The Physical Volcanology of Mars, in *Mars*, Kieffer, H.H., Jakosky, B.M., Snyder, C.W., and Matthews, M.S., Eds., Tucson: Univ. of Arizona Press, 1992, pp. 424–452.

Murphy, J.R., Wilson, G.W., Seiff, A., *et al.*, Meteorological Results from the *Mars Pathfinder* Lander: An Overview, *Lunar Planet. Sci. Conf. XXIX*, 1998, Abstract no. 1824.

Murhy, J.R., The Martian Atmospheric Dust Cycle: Insights from Numerical Simulations, *5th Int. Conf. on Mars*, July 19–24, 1999, Pasadena, CA, 1999, Abstract no. 6087.

Nelson, D.M. and Greeley, R., Geology of Xanthe Terra Outflow Channels and *Mars Pathfinder* Landing Site, *J. Geophys. Res.*, 1999, vol. 104, no. E4, pp. 8653–8669.

Nemchinov, I.V. and Shuvalov, V.V., Explosion Dynamics in Meteor Impacts on the Surface of Mars, *Astron. Vestn.*, 1992, vol. 26, no. 4, pp. 19–31.

Nemtchinov, I.V., Ivanov, B.A., Kozlov, I.M., *et al.*, Contamination of Earth's Atmosphere by Dust Particles Ejected after the Impact of Small Comets and Asteroids, in *Hazards due to Comets and Asteroids*, Tucson, Arizona, USA, January 4–9, 1993, p. 59.

Nemtchinov, I.V., Svetsov, V.V., Kosarev, I.B., *et al.*, Assessment of Kinetic Energy of Meteoroids Detected by Satellite-based Light Sensors, *Icarus*, 1997, vol. 130, no. 2, pp. 259–274.

Nemtchinov, I.V., Shuvalov, V.V., Artem'eva, N.A., *et al.*, Light Flashes Caused by Impacts against the Moon, in *CP429, Shock Compression of Condensed Matter—1997*, Schmidt, S.C., Dandekar, D.P., and Forbes, J.W., Eds., Woodbury, New York: AIP Conf. Proc. 429, 1998a, pp. 957–959.

Nemtchinov, I.V., Shuvalov, V.V., Artem'eva, N.A., *et al.*, Light Flashes Caused by Meteoroid Impacts on the Lunar Surface, *Astron. Vestn.*, 1998, vol. 32, no. 2, pp. 116–132 [*Sol. Syst. Res.* (Engl. transl.), 1998b, vol. 32, no. 2, pp. 99–114].

Nemtchinov, I.V., Popova, O.P., and Teterev, A.V., Intrusion of Large Meteoroids into the Atmosphere: Theory and Observations, *Inzh.-Fiz. Zh.*, 1999a, vol. 72, no. 6, pp. 1233–1265.

Nemtchinov, I.V., Popova, O.P., Rybakov, V.A., and Shuvalov, V.V., Initiation of Sandstorms due to Impacts of the 1–10 m-diameter Meteoroids onto the Surface of Mars, *5th Int. Conf. on Mars*, July 19–24, 1999, Pasadena, CA, 1999b, Abstract no. 6081.

Nemtchinov, I.V., Kosarev, I.B., Losseva, T.V., and Shuvalov, V.V., Radiation Impulse Caused by Impact of a Meteoroid onto Mars, 2000 Fall Meeting. *EOS, Transactions, AGU*, 2000, vol. 81, no. 48, Abstract P21A-07, F808.

Nemtchinov, I.V., Shuvalov, V.V., and Greeley, R., Impact Produced and Mobilized Dust in the Martian Atmosphere, 2000 Fall Meeting. *EOS, Transactions, AGU*, 2001, vol. 82, no. 47, Abstract P31A-0535.

Neukum, G. and Ivanov, B.A., Crater Size Distributions and Impact Probabilities on Earth from Lunar, Terrestial-Planet, and Asteroid Cratering Data, in *Hazards due to Comets and Asteroids*, Gehrels, T., Ed., Tucson: Univ. of Arizona Press, 1994, pp. 359–416.

Olsson–Steel, D., Collisions in the Solar System. IV. Cometary Impacts upon the Planets, *Mon. Not. R. Astron. Soc.*, 1987, vol. 227, no. 2, pp. 501–524.

Owen, T., The Composition and Early History of the Atmosphere of Mars, in *Mars*, Kieffer, H.H., Jakosky, B.M., Snyder, C.W., and Matthews, M.S., Eds., Tucson: Univ. of Arizona Press, 1992, pp. 818– 834.

Parker, T.J. and Rice, J.W., Jr., Sedimentary Geomorphology of the *Mars Pathfinder* Landing Site, *J. Geophys. Res.*, 1997, vol. 102, no. E11, pp. 25641–25656.

Parsons, J.D., Are Fast Growing Martian Dust Storms Compressible? *Geophys. Res. Lett.*, 2000, vol. 27, no. 15, pp. 2345–2348.

Pollack, J.B., Kasting, J.F., Richardson, S.M., and Poliakoff, K., The Case for a Wet, Warm Climate on Early Mars, *Icarus*, 1987, vol. 71, pp. 203–224.

Rennó, N.O., Burkett, M.L., and Larkin, M.P., A Simple Thermodynamical Theory for Dust Devils, *J. Atmos. Sci.*, 1998, vol. 55, pp. 3244–3252.

Ryan, J.A. and Lucich, R.D., Possible Dust Devils, Vortices on Mars, *J. Geophys. Res.*, 1983, vol. 88, pp. 11005–11011.

Rybakov, V.A., Nemtchinov, I.V., Shuvalov, V.V., *et al.*, Mobilization of Dust on the Mars Surface by the Impact of Small Cosmic Bodies, *J. Geophys. Res.*, 1997, vol. 102, no. E4, pp. 9211–9220.

Scchfield, J.T., Barnes, J.R., Crisp, D., *et al.*, The MPF Atmospheric Structure Investigation/Meteorology (ASI/MET) Experiment, *Science*, 1997, vol. 278, pp. 1752–1758.

Schultz, P.H., Atmospheric Effects on Ejecta Emplacement, *J. Geophys. Res.*, 1992, vol. 97, pp. 11623–11662.

Schultz, P.H. and Gault, D.E., Atmospheric Effects on Martian Ejecta Emplacement, *J. Geophys. Res.*, 1979, vol. 84, pp. 7669–7687.

Shuvalov, V.V., Multidimensional Hydrodynamic Code SOVA for Interfacial Flows: Application to Thermal Layer Effect, *Shock Waves*, 1999, vol. 9, no. 6, pp. 381–390.

Shuvalov, V.V., Artemieva N.A., and Kosarev, I.B., 3D Hydrodynamic Code SOVA for Multimaterial Flows: Application to Shoemaker–Levy 9 Comet Impact Problem, *Int. J. Impact Engng.*, 1999, vol. 23, pp. 847–858.

Shuvalov, V.V. and Artemieva, N.A., Atmospheric Erosion and Radiation Impulse Induced by Impacts, in *Catastrophic Events and Mass Extinction: Impacts and Beyond*, Houston: LPI, 2000, LPI Contribution no. 1053, pp. 199–200.

Solov'ev, S.P. and Shuvalov, V.V., Dynamical Processes at Strong TNT Explosions, in *Fizicheskie processy v geosferakh: ikh proyavleniya i vzaimodeistvie (Geofizika sil'nykh vozmushchenii)* (Physical Processes in Geospheres: Their Manifestation and Interaction (Geophysics of Strong Disturbances), Moscow: IGD (Inst. of Geosphere Dynamics), 1999, pp. 369–377.

Squyres, S.W., Clifford, S.M., Kuzmin, R.O., *et al.*, Ice in the Martian Regolith, in *Mars*, Kieffer, H.H., Jakosky, B.M., Snyder, C.W., and Matthews, M.S., Eds., Tucson: Univ. of Arizona Press, 1992, 523–554.

Steel, D., Collisions in the Solar System: II. Asteroid Impacts upon Mars, *Mon. Not. R. Astron. Soc.*, 1985, vol. 215, no. 3, pp. 369–381.

Stewart, S.T., O'Keefe, J.D., and Ahrens, T.J., The Role of Subsurface Ice and Water in Rampart Crater Formation, 2000 Fall Meeting. *EOS, Transactions, AGU*, 2000, vol. 81, no. 48, Abstract P62C-03, F783.

Strom. R.G., Croft, S.K., and Barlow, N.G., The Martian Impact Cratering Record, in *Mars*, Kieffer, H.H., Jakosky, B.M., Snyder, C.W., and Matthews, M.S., Eds., Tucson: Univ. of Arizona Press, 1992, 383–423.

Tagliaferri, E., Spalding, R., Jacobs, C., *et al.*, Detection of Meteoroid Impacts by Optical Sensors in Earth Orbit, in *Hazards due to Comets and Asteroids*, Gehrels, T., Ed., Tucson: Univ. of Arizona Press, 1994, pp. 199–220.

Teterev, A.V., Cratering Model of Asteroid and Cometary Impact on a Planetary Surface, *Int. J. Imact Engng.*, 1999, vol. 23, pp. 921–932.

Thomas, P.C. and Gierasch, P.J., Dust Devils on Mars, *Science*, 1985, vol. 230, pp. 175–177.

Thompson, P.C. and Lauson, H.S., Improvements in the Chart D Radiation–Hydrodynamic CODE III: Revised Analytic Equations of State, Prepared by Sandia Laboratories, Albuquerque, NM 87115 and Livermore, CA

94550 for the US Atomic Energy Commission under Contract AT(29-1)-789. Report SC-RR-71 0714, 1972.

Trubetskaya, I.A. and Shuvalov, V.V., Numerical Simulation of Contamination of the Environment by Radioactive Dust from Nuclear Tests, in *Fizicheskie processy v geosferakh: geofizika sil'nykh voznushchenii* (Physical Processes in Geospheres: Geophysics of Strong Disturbances), Moscow: Nauka, 1994, pp. 249–259.

Vickery, A.M. and Melosh, H.J., Atmospheric Erosion and Impactor Retention in Large Impacts with Application to Mass Extinctions, in *Global Catastrophes in Earth History*, Sharpton, V.L. and Ward, P.D., Eds., Geol. Soc. Am. SP-247, 1990, pp. 289–300.

Ward, W.R., Large-Scale Variations in the Obliquity of Mars, *Science*, 1973, vol. 181, pp. 260–262.

Ward, W.R., Murray, B.C., and Malin, M.C., Climatic Variations on Mars, *J. Geophys. Res.*, 1974, vol. 79, pp. 3387–3395.

Zahnle, K.J., Xenological Constraints on the Impact Erosion of the Early Martian Atmosphere, *J Geophys. Res.*, 1993, vol. 98, no. E6, pp. 10899–10913.

Zeldovich, Ya.B. and Raizer, Yu.P., *Fizika udarnykh voln i vysokotemperaturnykh gidrodinamicheskikh yavlenii, Moscow: Nauka, 1966 [Physics of Shock Waves and High-Temperature Hydrodynamic Phenomena* (English transl.), San Diego: Academic, 1966].

Zurek, R.W., Comparative Aspects of the Climate of Mars: An Introduction to the Current Atmosphere, in *Mars*, Kieffer, H.H., Jakosky, B.M., Snyder, C.W., and Matthews, M.S., Eds., Tucson: Univ. of Arizona Press, 1992, pp. 799–817.